AIAA JOURNAL
Vol. 32, No. 11, November 1994

Effects of Expansions on a Supersonic Boundary Layer: Surface Pressure Measurements

Jonathan A. Dawson,* Mo Samimy,† and Stephen A. Arnette‡
Ohio State University, Columbus, Ohio 43210

Multipoint wall pressure measurements are used to investigate the response of a Mach 3, fully developed, compressible, turbulent boundary layer ($Re\theta \simeq 25{,}000$) to centered and gradual ($R/\delta \simeq 50$) expansions, both of 7- and 14-deg deflection. Although rms fluctuation levels decrease across the expansions, the rms normalized by the local static pressure remains nominally constant. Just downstream of the expansions, normalized power spectra are more concentrated at low frequencies ($f <$ 10–15 kHz) than upstream, suggesting small-scale turbulence is quenched. This spectra alteration is more prominent for centered expansions and larger deflections. The spectra evolve very quickly after the centered expansions and very slowly after the gradual expansions. Downstream of the expansions, space-time correlations do not lend themselves to the derivation of convection velocities, signifying a severe distortion of the boundary layers. Measurements immediately after the gradual expansions compare well with those further downstream of the centered expansions of the same deflection, suggesting the distance from the beginning of the expansions is the appropriate length scale for characterizing the boundary-layer evolution. After the expansions, a band of elevated spanwise coherence (around 15–30 kHz) and elevated spanwise correlation levels emerge. Increases in streamwise coherence and correlation are less pronounced. At the last measurement stations, the boundary layers remain far from equilibrium.

Nomenclature

P = mean static pressure
R = radius of curvature of gradual expansion
U = mean velocities in the streamwise direction
V = mean velocities in the normal direction
x = streamwise direction
y = normal direction
z = spanwise direction
Δx = streamwise transducer spacing
Δz = spanwise transducer spacing
δ = boundary-layer thickness
ρ = density
σ_P = rms pressure fluctuations

Subscripts

L = local value
0, 1 = value before the expansion
2 = value after the expansion
θ = based on momentum thickness

I. Introduction

FLAT plate, compressible, turbulent boundary layers have been studied for decades. However, in practical situations, compressible boundary layers are typically influenced by streamline curvature, bulk dilatation or compression, pressure gradients, and other complexities. These effects define a larger class of complex turbulent flows that possess "extra rates of strain." Extra rates of strain are defined as velocity gradients that exist in addition to the dominant $\partial U/\partial y$ boundary-layer gradient.[1] A summary of the current knowledge of perturbed, compressible turbulent boundary layers is given by Spina et al.[2]

In passing through an expansion, the compressible turbulent boundary layer is subjected to a favorable pressure gradient (and the associated bulk dilatation) and convex streamline curvature. There have been several investigations of compressible turbulent boundary layers subjected to favorable pressure gradients in the absence of convex streamline curvature[2]. Bradshaw[1] found the effects of pressure gradients on supersonic flows to be significantly underestimated by an order-of-magnitude analysis of the turbulence equations. Morkovin[3] found longitudinal turbulence intensities to be decreased significantly by a favorable pressure gradient. It has also been demonstrated that the induced bulk dilatation serves to decrease the wall shear stress and increase the boundary-layer thickness. Although preceded by a region of adverse pressure gradient, the outer edge of the Mach 2.5 turbulent boundary layer of Lewis et al.[4] subjected to a favorable pressure gradient corresponded approximately to a streamline, signifying a suspension of freestream fluid entrainment into the boundary layer. These observations show the favorable pressure gradient to be stabilizing; i.e., the turbulence's ability to transport momentum to the wall or entrain fresh fluid is decreased.

Convex streamline curvature in a compressible flow is normally accompanied by a favorable pressure gradient (as in this study). However, convex curvature can be isolated from the associated pressure gradients by introducing appropriate concave streamline curvature on an opposing solid boundary. Such an investigation was performed by Thomann[5] in studying the effect of streamline curvature on wall heat transfer for an incoming Mach 2.5 turbulent boundary layer. Gradual convex curvature of 20 deg resulted in a decrease in the wall heat transfer of approximately 15–20% relative to the flat plate levels. Gradual concave curvature of 20 deg resulted in a similar percent increase. This shows convex curvature to also be stabilizing; i.e., the turbulence's ability to transport low-temperature, freestream fluid into the near-wall region is reduced.

As mentioned, the compressible turbulent boundary layer is subjected to both convex streamline curvature and a favorable pressure gradient in negotiating an expansion region. Given the nonlinear response of the turbulent boundary layer to extra rates of strain, there is no reason to expect the boundary-layer response to represent a simple superposition of the effects induced individually by streamline curvature and pressure gradients.

Dussauge and Gaviglio[6] investigated a 12-deg centered expansion of a Mach 1.8 equilibrium turbulent boundary layer (δ = 10 mm, Re_θ = 5000). Hot-wire measurement of longitudinal velocity and temperature fluctuations were acquired. Across the expansion, longitudinal turbulence intensities were reduced through the entire

Received July 24, 1993; revision received May 2, 1994; accepted for publication May 2, 1994.

*Graduate Student, Department of Mechanical Engineering.
†Professor, Department of Mechanical Engineering. Associate Fellow AIAA.
‡Graduate Student, Department of Mechanical Engineering. Student Member AIAA.

boundary-layer thickness. The reductions were small for $y/\delta > 0.7$ but became more substantial closer to the boundary. Calculations based on rapid distortion theory that accounted for the effect of bulk dilatation reproduced the reductions in longitudinal turbulence intensity very well in the outer portions of the boundary layer. However, the more significant reductions near the wall were not fully captured by the calculations. The evolution of the mean velocity profile downstream of the expansion is very similar to that of Lewis et al.[4] for a flat plate boundary layer subjected to a favorable pressure gradient. The logarithmic region of the mean velocity profile was destroyed across the 12-deg expansion and did not reappear until approximately 10δ downstream of the expansion corner. At this location, longitudinal Reynolds stress profiles remained well below equilibrium levels. The turbulence recovery originated near the wall, progressively occupying more of the boundary-layer thickness. Thus it was concluded that a new wall layer was formed and that the boundary layer had relaminarized. Dussauge[7] proposed a description for the relaminarization process and identified two zones of influence: an outer zone where slow variations occur and an inner zone where turbulence is re-formed.

For incompressible turbulent boundary layers, it has been shown that a sufficiently favorable pressure gradient can cause relaminarization.[8] Reversion of the mean flow is said to be completed when the net effect of the Reynolds stresses is negligible. Narasimha and Viswanath[9] suggest relaminarization occurs after an expansion corner if $\Delta P/\tau_0 > 70$–75, where ΔP is the pressure drop across the expansion and τ_0 is the surface shear stress before the expansion.

Smith and Smits[10] studied a 20-deg centered expansion of a Mach 2.84 boundary layer ($\delta = 26$ mm, $Re_\theta = 77{,}600$). Measurements 3.5δ downstream of the expansion corner compared favorably with those of Dussauge and Gaviglio.[6] No logarithmic region was evident in the mean velocity profile, and both the longitudinal turbulence intensity and Reynolds stress were significantly reduced. Calculations similar to those of Dussauge and Gaviglio[6] were performed with similar success. Interestingly, the mass-flux fluctuation profile was not altered significantly through the expansion. Thus, although the published criterion for relaminarization had been met, caution was urged in using the term.

As highlighted by Spina et al.,[2] these studies of expanded compressible turbulent boundary layers demonstrate the effects of bulk dilatation more than those of surface curvature since, for these two-dimensional flows, $\partial U/\partial x + \partial V/\partial y >> \partial V/\partial x$. This disparity should be enhanced with increasing Mach number.

Using the same expansion models and tunnel as in this study, Arnette et al.[11] used filtered Rayleigh scattering to investigate the effects of expansions on the Mach 3 turbulent boundary layer. Streamwise-elongated structures were found to populate the upper half of the boundary layer before and after the expansion regions. The planar visualizations, in which the freestream was marked with a condensation tracer, did not permit visualizations deeper in the boundary layer. A discussion of these structures in the flat plate boundary layer is given by Samimy et al.[12] Arnette et al.[11] found the large-scale structures of the outer layer maintained their identity and increased in scale across the expansions and the structure angle also appeared to increase. The visual prominence of the large-scale structures was enhanced across the expansions due to more significant penetrations of marked potential fluid into the boundary layer, suggesting small-scale motions were quenched. This observation seems to agree with the results of Dussauge and Gaviglio[6] and Smith and Smits,[10] where sharp reductions in near-wall turbulence were encountered across the expansions.

The present work studies the effect of varying degrees and rates of expansion on a Mach 3 turbulent boundary layer. The four expansion cases consist of centered expansions of 7 and 14 deg and gradual expansions ($R/\delta \simeq 50$) of 7 and 14 deg.

II. Experimental Setup

The experiments were performed at the Ohio State University Aeronautical and Astronautical Research Laboratory. Compressed dry air is provided by two four-stage compressors and stored in tanks with a capacity of 42.5 m^3 at pressures up to 16.4 MPa. Air is delivered to the tunnel through an array of radial inlet holes, and the stagnation pressure is adjusted with a pneumatically controlled ball valve. The stagnation pressure was 1.14 MPa, and the stagnation temperature was nominally 280 K. The incoming supersonic flow occupies a passage 152.4 mm wide and 76.2 mm tall at the beginning of the expansion regions, after which the cross-sectional area of the passage increases. The boundary layer develops on a flat plate from the stagnation chamber to the beginning of the expansions (67 cm from the nozzle throat to the beginning of the expansions), and transition is natural. The one-sided nozzle contour is opposite the flat plate surface. Previous laser Doppler velocimetry (LDV) measurements have shown the streamwise and normal freestream turbulence intensities are less than 3%.[13] At the location of the beginning of the expansion regions, the LDV results showed $M_\infty = 3.01$, $\theta = 0.37$ mm, $Re_\theta = 24{,}700$, and $\delta_0 = 9.2$ mm.

Schematics of the expansion models are shown in Fig. 1. For the centered expansion models (Fig. 1a), the flat plate boundary layer experiences a 7- or a 14-deg expansion corner. For the gradual expansion models (Fig. 1b), the flat plate boundary layer experiences 7 or 14 deg of gradual convex surface curvature ($R = 450$ mm). It has been shown for gradual concave curvature that the effects on the boundary layer vary with R/δ.[14,15] Given this, a large value of R/δ (≈ 50) was used with expectations that differences would arise between the centered and gradual expansions of the same total deflection. The regions of gradual surface curvature have a streamwise extent of 55 mm ($6\delta_0$) and 110 mm ($12\delta_0$) for the 7- and 14-deg gradual expansions, respectively. As in Fig. 1, the streamwise coordinate x is measured along the model surface with the origin at the beginning of the expansions. The previously measured δ_0 is used to normalize the streamwise coordinate. Pertinent ratios across the expansions obtained from an inviscid analysis are given in Table 1.

Static pressure information was acquired from static taps in the models with a 12-port Scanivalve. Measurements were made in both the spanwise and streamwise directions with a distance between static taps of 12.7 mm ($1.4\delta_0$). The streamwise static taps were offset from the model centers by 19.1 mm ($2.1\delta_0$) so as to not interfere with the centered transducers.

Table 1 Ratio across expansions from inviscid analysis

Total deflection, deg	7	14
Mach number, M_2	3.40	3.86
Velocity ratio, U_2/U_1	1.05	1.08
Pressure ratio, P_2/P_1	0.56	0.30
Density ratio, ρ_2/ρ_1	0.66	0.42

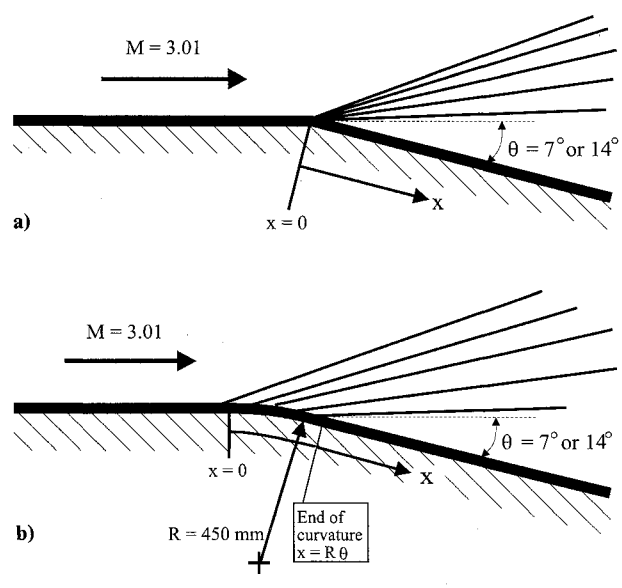

Fig. 1 Schematics of the a) centered and b) gradual expansion models.

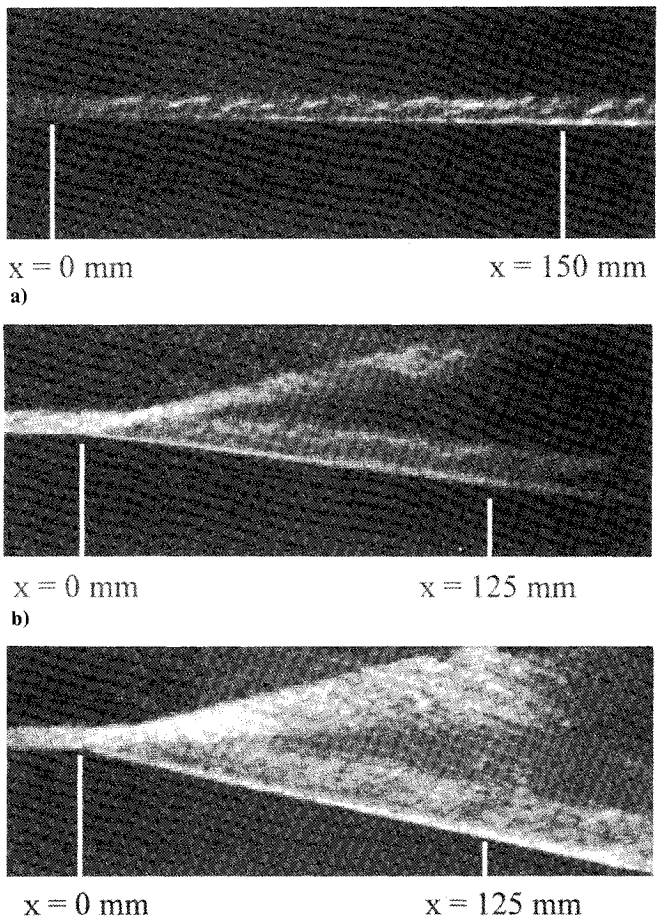

Fig. 2 Instantaneous schlieren images of the a) flat plate, b) 7-deg centered, and c) 14-deg centered expansion boundary layers.

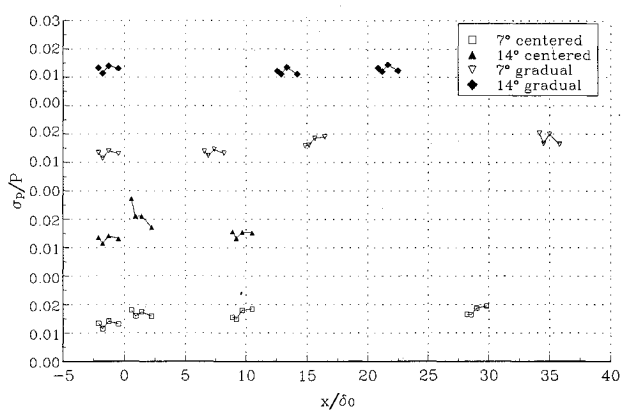

Fig. 3 Normalized rms pressure fluctuations for all four expansion models and the incoming boundary layer (the results for different models are staggered vertically).

The instantaneous pressure data were acquired with four fast-response Endevco pressure transducers (Model 8514-10) powered by an Ectron model 563F signal conditioner. The transducers were statically calibrated against a mercury manometer. Previous work has shown the difference between the static and dynamic calibrations is only a few percent for these types of transducers (see, for example, Tan et al.[16] or Fernholz et al.[17]). The gain was set so as to match the output of the transducers under maximum pressure differential to the ±10 V range of the analog-to-digital (A/D) converter.

The transducer diaphragm (diameter of approximately 1 mm) is recessed below a cover containing pinholes. Corcos[18] demonstrated that the response of a transducer is valid up to a nondimensional frequency of $2\pi fr/U_c \approx 1.0$, where f is the maximum valid

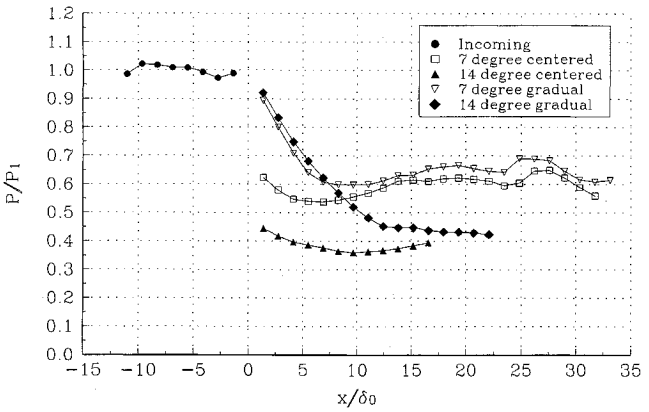

Fig. 4 Streamwise distribution of static pressure at the model surfaces, $P_1 = 22$ kPa.

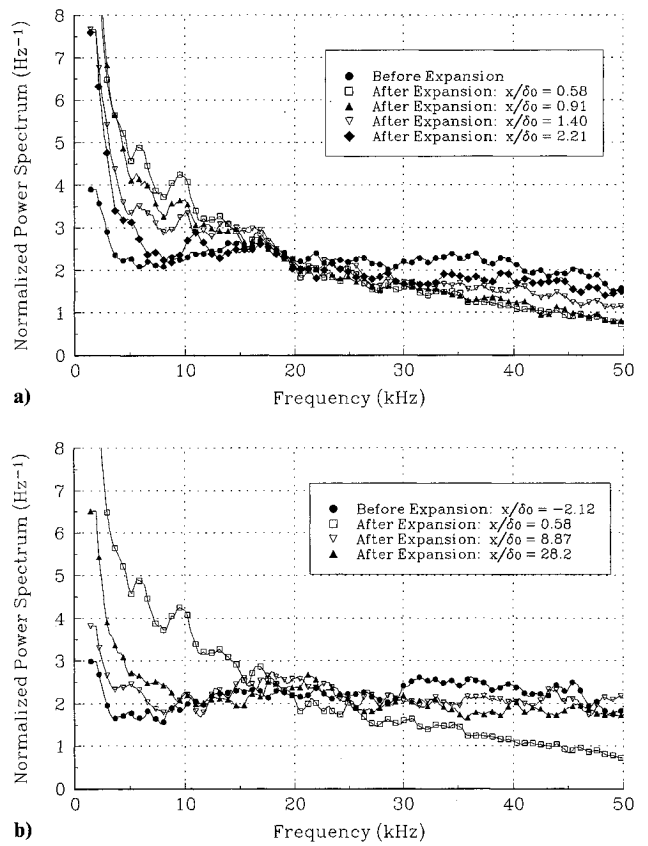

Fig. 5 Normalized power spectra downstream of the 7-deg centered expansion: a) immediately after the expansion and b) downstream evolution.

frequency, r is the diaphragm radius, and U_c is the measured convection velocity. If the convection velocity of the structures is approximately 90% of the freestream value (as found by Spina et al.[19]) of about 600 m/s obtained previously in this tunnel with LDV,[13] $f \approx 168$ kHz. However, the resonation of the transducer cavity appeared to corrupt the data above about 70 kHz. As a result, the data were low-pass filtered at 60 kHz. To eliminate low-frequency noise, a high-pass filter was applied at 1 kHz. The transducers were mounted in an aluminum plug that fit into holes located on the model centerlines. Since the plug is circular, the transducers can be skewed at any angle to the flow direction. For this work, only streamwise and spanwise orientations were employed.

The data were acquired using a Datel PC414-A2 12-bit A/D converter board and accompanying software (PC414-SET). The A/D converter was equipped with a simultaneous sample and hold

module that allowed data on all four channels to be sampled at the same time, thereby negating any phase difference between the signals. Data were collected simultaneously at the four locations at a sampling rate of 250 kHz per channel. Subjecting the four transducers to identical pressure signals confirmed that no artificial phase shifts between different channels were present in the system. A data set contained 51,200 data points per channel. This system has a mean sensitivity of approximately 60 Pa per bit with A/D fluctuations of approximately ±1 bit at constant pressure. All data were stored and subsequently processed on a 486 PC. Data filtering and analysis were performed with MATLAB software and the accompanying Signal Processing Toolbox. The power spectral analyses were performed with 100 sets of 1024 data points, and correlations were performed with 50 sets of 1024 data points. Full details of the data analysis are given by Dawson.[20]

Flow visualization was performed using a standard schlieren setup. Images were collected with an ICCD camera and recorded on Super-VHS. The photographs were used both to check for freestream uniformity and to obtain measurements of the boundary layer thickness.

III. Results and Discussion

As can be seen in Fig. 2, where instantaneous (light pulse duration of 10 ns) schlieren images of the flat plate and centered expansion cases are shown, the boundary layer thickens substantially across the expansion regions. Measurements from average schlieren images indicate the boundary-layer thickness increases approximately 150% across the 7-deg expansions and 200% across the 14-deg expansions. Calculations based on the expansion of an incoming power-law velocity profile to the inviscid density ratios in which zero entrainment through the expansion is assumed (as suggested by the measurements of Lewis et al.[4]) indicate a boundary-layer thickening of 12–14% less than that estimated from the schlieren images. Given the increase in boundary-layer thickness across the expansions, the use of δ_0 as a global length scale is less than ideal.

Using the method of Narasimha and Viswanath,[9] $\Delta P/\tau_0$ is estimated to be 48 and 76 for the 7- and 14-deg expansions, respectively. Since the favorable pressure gradient is less severe for the the gradual expansion, the 14-deg centered expansion is the only one considered close to relaminarization. Figure 3 gives the normalized rms pressure fluctuations for the incoming and four expansion boundary-layer cases. The rms values are normalized by the average of the mean pressures recorded by the four adjacent transducers at each measurement station. The σ_P/P of 0.013 in the incoming boundary layer compares very favorably to the value of 0.014 obtained by Muck et al.[21] in a Mach 2.9 high-Reynolds-number, turbulent boundary layer. The normalized levels increase initially across the centered expansions. Further downstream the levels compare well with those of the flat plate boundary layer. This shows significant turbulent fluctuations to persist downstream of the expansions, which does not give an indication of relaminarization (even for the 14-deg centered expansion). The fact that the streamwise mass-flux fluctuations in a Mach 2.84 boundary layer did not change appreciably across a 20-deg expansion led Smith and Smits[10] to caution against the term relaminarization. The variations for adjacent transducers far downstream of the expansions are probably due to the slightly different dynamic responses of individual transducers since the static transducer calibration was repeated several times during the data collection to insure reliable results.

The streamwise distribution of mean static pressure at the model surfaces (both upstream and downstream of the four expansions) is shown in Fig. 4. Nonuniformities in the streamwise (Fig. 4) and spanwise (given by Dawson[20]) distributions in the incoming boundary layer correspond to a peak-to-peak Mach number variation of only 0.03. Spanwise distributions downstream of the four expansions were collected at a distance of $3.65\delta_0$ downstream of the end of the surface curvature (given by Dawson[20]). Downstream of the 14-deg expansions ($M_\infty \simeq 3.86$, see Table 1), variation magnitudes at these locations are similar to those found in the incoming boundary layer. Downstream of the 7-deg expansions ($M_\infty \simeq 3.40$), the spanwise variations correspond to a peak-to-peak Mach number variation of 0.18.

The measured pressure ratios (P_2/P_1) across the 7-deg expansion models are very close to those obtained from an inviscid Prandtl-Meyer analysis (Table 1), but the measured ratios for both 14-deg models are higher than the inviscid ratios. Smith and Smits[10] also measured a higher pressure ratio than the inviscid ratio for a 20-deg centered expansion in a Mach 2.84 flow. Pressure ratios calculated using the hypersonic similarity parameter[22] are 0.33 for the 14-deg and 0.59 for the 7-deg expansions, which are slightly lower than those of Fig. 4. For the centered expansions, the pressure reaches a minimum in $5–10\delta_0$ and then gradually increases.

A. 7-Deg Centered Expansion

Significant development of the power spectrum (normalized by $\sigma_P^2/125{,}000$) of the pressure fluctuations occurs over a short streamwise distance immediately after the 7-deg centered expansion. Figure 5a shows that the first stage consists of a shift of the spectral density to low frequencies ($f < 15$ kHz) and a corresponding decrease at higher frequencies (recall that the normalized spectra reflect only the spectral distribution of the fluctuation "energy"). The elevated low-frequency levels then begin to decrease, whereas the broad range of higher frequencies recovers more slowly. At these same positions, streamwise coherence levels in the low-frequency range drop from above to below those of the incoming boundary layer as the transducer spacing increases from $0.33\delta_0$ to $1.63\delta_0$, whereas little change occurs for higher frequencies. This again suggests that rapid development occurs just after the expansion.

The downstream power spectra show the pressure spectra to approach and then to begin to move away from the flat plate distribution (Fig. 5b). Since there is a distance of about $20\delta_0$ between the two downstream measurement locations, it is quite possible that the low-frequency levels drop below those of the flat plate boundary layer between these two stations. Whether or not this is true, there is clearly not a monotonic recovery to the flat plate spectrum.

An interesting observation arises downstream. The last two measurement stations in Fig. 6 show bands of elevated spanwise coherence relative to the flat plate boundary layer centered near 20 kHz. This might indicate organized structures in the flow that were not present before the expansion. If this were the case, the significant increase in coherence level between $x/\delta_0 = 9.52$ and 28.8 would signify increasing spanwise extent and/or organization with downstream distance. Interestingly, the streamwise coherence at these locations shows only slight increases.

The correlation results show a slight increase in the peak streamwise correlation downstream (Fig. 7a) but a significant increase in the peak spanwise correlation (Fig. 7b). The increases in coherence and correlation levels seem to suggest these new structures have larger spanwise extent and greater spanwise organization than in the incoming boundary layer. It is again noted that in the presented graphs, the transducer spacings are normalized by the incoming boundary-layer thickness. Although the increase in

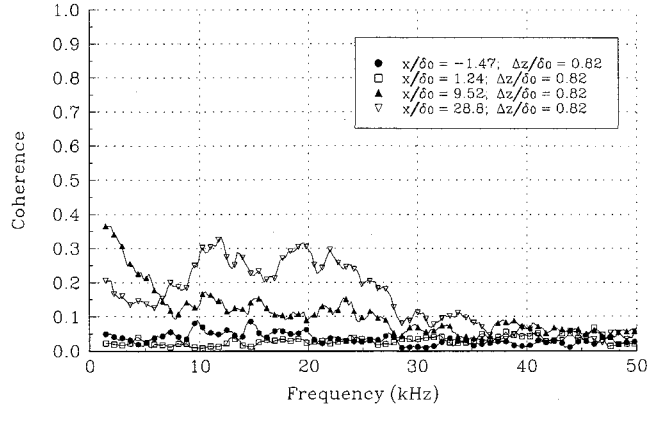

Fig. 6 Spanwise coherence downstream of the 7-deg centered expansion.

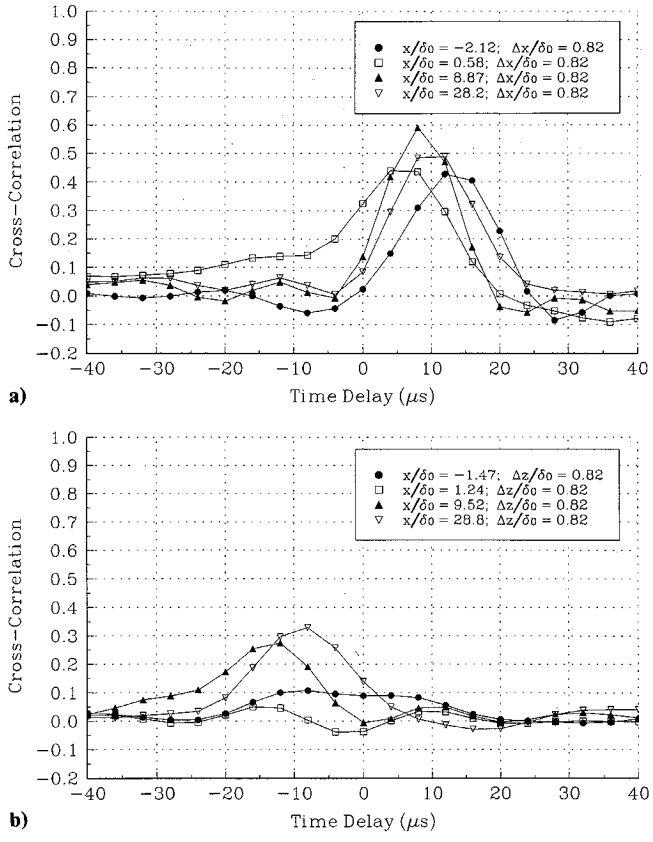

Fig. 7 Space-time correlations downstream of the 7-deg centered expansion: a) streamwise and b) spanwise.

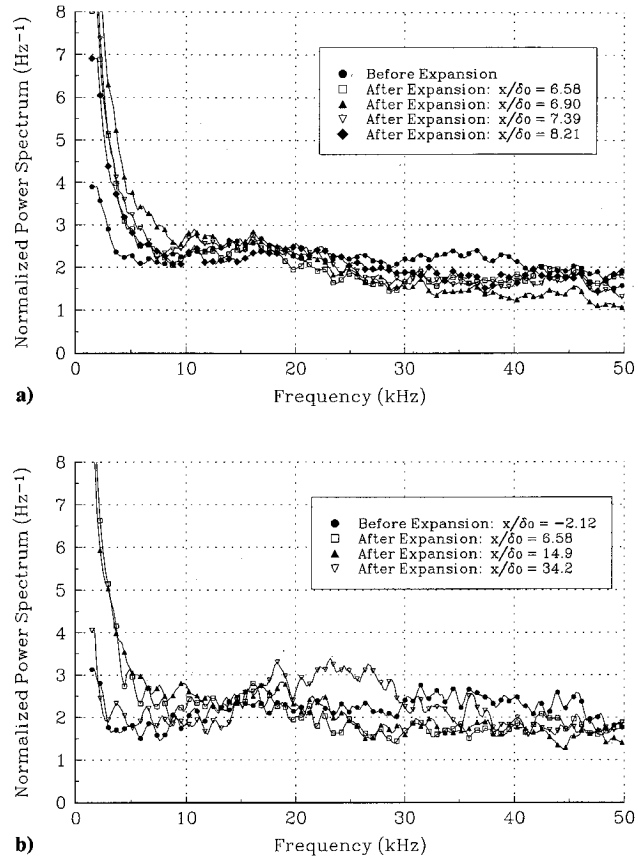

Fig. 8 Normalized power spectra downstream of the 7-deg gradual expansion: a) immediately after the expansion and b) downstream evolution.

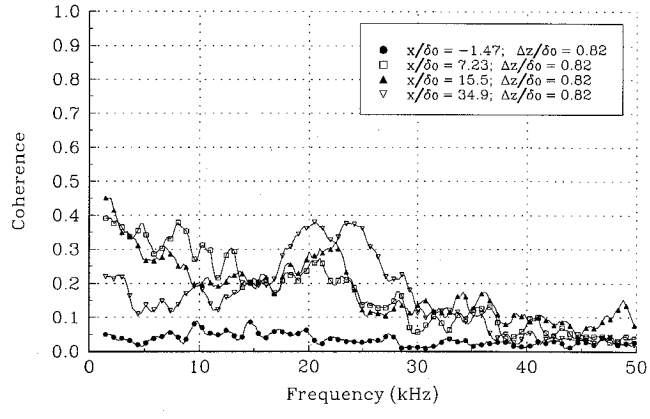

Fig. 9 Spanwise coherence downstream of the 7-deg gradual expansion.

boundary-layer thickness across the expansion might partially account for the higher coherence and correlation levels after the expansion, it is shown later that this is not the primary explanation.

The most common use of the space-time correlation is in the identification of a convection velocity U_c. If it is assumed that the turbulence is not rapidly changing (Taylor's frozen field hypothesis), then the time delay at peak correlation level is a measure of the average time it takes for coherent motions to traverse the probe separation. In Fig. 7, the time resolution of the four-channel measurements (4 μs) is not sufficient for an accurate measurement of the convection velocity. For the incoming boundary layer only, two-channel data were acquired at 500 kHz per channel to increase the time resolution from 4 to 2 μs. With those data, convection velocities of 80–90% of the freestream velocity measured by Samimy et al.[12] were obtained, in agreement with the current literature.[19] A value of $0.9U_\infty$ is obtained by interpolating a peak at $\Delta t = 14$ μs in Fig. 7. Furthermore, as expected in the two-dimensional flat plate boundary layer, the spanwise space-time correlations were symmetric about $\Delta t = 0$ for $\Delta z/\delta_0 = 0.33$ and displayed negligible correlation for $\Delta z/\delta_0 = 0.82$ (Fig. 7b) and 1.63. In addition to these results, other tests confirmed that no artificial phase delays existed between the transducers (e.g., switching the transducer order did not affect the results).

The convection velocities indicated by the streamwise correlations after the expansion regions are unreasonably high. The spatial simulation of supersonic turbulence by Lee et al.[23] showed that if one performed a space-time correlation of dilatation fluctuations (which are closely related to pressure fluctuations), convection velocities greater than the actual propagation velocities would be obtained. This is due to the propagation of acoustic disturbances with the acoustic velocity relative to the local velocity. It should also be noted that Arnette et al.[24] have obtained large ensembles of double-pulse, instantaneous visualizations downstream of this 7-deg centered expansion and performed two-dimensional space/time correlations for the purpose of obtaining convection velocities. The results show that the visual features commonly identified as large scale eddies convect at a velocity slightly less than the freestream velocity downstream of the expansion (obtained from an inviscid analysis assuming the flat plate freestream velocity measured by Samimy et al.[13]). Thus it appears that space-time correlations of fluctuating surface pressures are not a suitable technique for determining convection velocities in these severely distorted boundary layers.

For the spanwise space-time correlations, there are notable shifts to negative time delays downstream of the expansions, which is very puzzling. Although one might conceive of some type of acoustically propagating disturbance giving rise to nonzero time shifts at maximum correlation, the lack of symmetry about $\Delta t = 0$ is very perplexing. Further downstream, the peak time delays move towards those of the incoming boundary layer for both streamwise and spanwise correlations, but the delays are still far off at the last measurement locations.

B. 7-Deg Gradual Expansion

The results of the 7-deg gradual expansion model demonstrate that just downstream of the end of the expansion region ($x/\delta_0 \simeq 7$) no rapid spectral development is occurring as for the 7-deg centered expansion but that a small shift to low-frequencies is still noticeable (Fig. 8a). This suggests the gradual curvature has allowed the boundary layer to adjust within the expansion. The low frequency spectral levels increase between $x/\delta_0 = 6.58$ and 6.90 and then progressively decrease at $x/\delta_0 = 7.39$ and 8.21, signifying a nonmonotonic spectral evolution. No measurements were made within the gradual expansion regions. Streamwise coherence results also demonstrate that the evolution after the gradual expansion is not rapid.

The 7-deg gradual expansion exhibits not only elevated spanwise coherence for $f = 15$–30 kHz but also elevated spectral densities at $x/\delta_0 = 34.2$ (Fig. 8b). None of the other postexpansion spectra displayed elevated spectral levels at these frequencies. Clearly, the feature giving rise to elevated coherence at 15–30 kHz is more prominent here than at any other measurement location for any other expansion. The broad spanwise coherence peak at 15–30 kHz in Fig. 9 offers further support. If some type of new "structural" feature is responsible, they are much more energetic than in the centered expansion cases. The correlations in Figs. 9a and 9b demonstrate again that although the spanwise extent is increased significantly, little identifiable increase has occurred in the streamwise direction.

Again, the space-time correlations (Fig. 10a) exhibit small time delays that produce unreasonable convection velocities. The spanwise correlations (Fig. 10b) are again nonsymmetric with large peaks at nonzero time delays. It appears that as the flow progresses downstream the correlation is beginning to evolve towards that of the flat plate boundary layer, although drastic differences are still present at the last measurement location. The time delays at peak correlation for the streamwise separations do not appear to approach those of the flat plate boundary layer with increasing downstream distance. Clearly, the state of the boundary layer at $x/\delta_0 = 34.2$ is very different than that of the flat plate boundary layer.

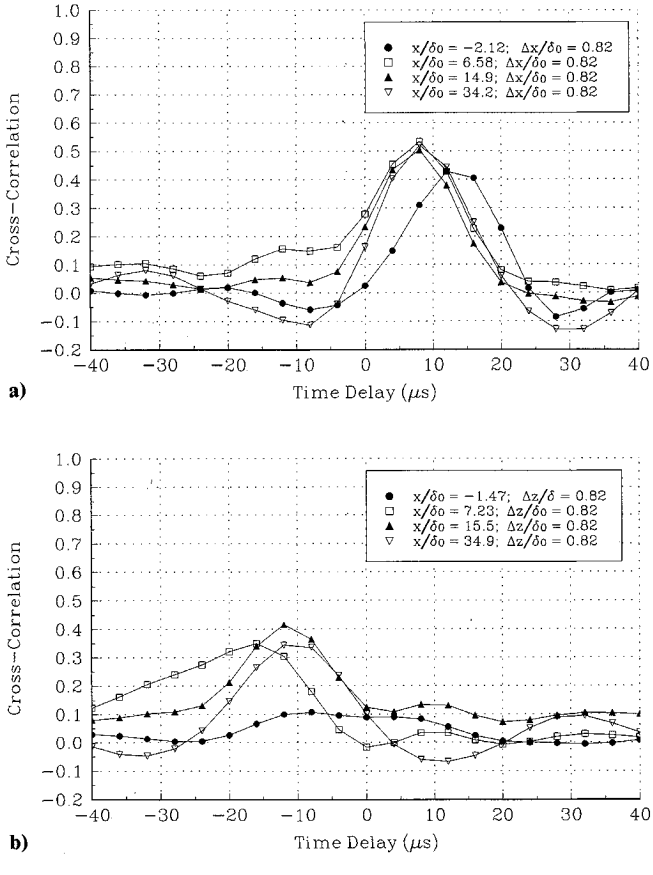

Fig. 10 Space-time correlations downstream of the 7-deg gradual expansion: a) streamwise and b) spanwise.

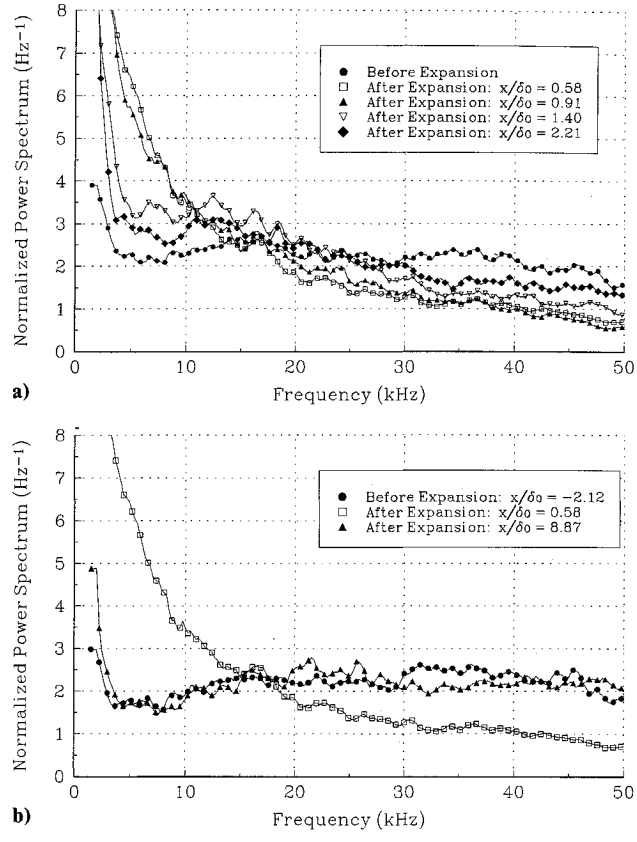

Fig. 11 Normalized power spectra downstream of the 14-deg centered expansion: a) immediately after the expansion and b) downstream evolution.

A fair comparison can be made between the pressure spectra (Figs. 5 and 8) and the spanwise coherence (Figs. 6 and 9) at $x/\delta_0 = 6.58$ for the 7-deg gradual model and $x/\delta_0 = 8.87$ for the 7-deg centered model, and likewise between $x/\delta_0 = 14.9$ for the 7-deg gradual model and $x/\delta_0 = 28.2$ for the 7-deg centered model. The spectra and spanwise coherence for the 7-deg gradual expansion at $x/\delta_0 = 34.2$ display higher levels at $f = 10$–30 kHz than are found at $x/\delta_0 = 28.2$ for the 7-deg centered expansion. The favorable comparison at the cited locations suggests the new features would emerge further downstream of the centered expansion. The earlier appearance of these features in the gradual case seems to indicate that the gradual curvature allows the turbulence to rearrange itself more efficiently through the expansion. Whether or not the overall length required for emergence (measured from the beginning of the expansion) changes cannot be commented on due to the limited model lengths.

C. 14-Deg Centered Expansion

The pressure fluctuation spectrum immediately after the 14-deg centered expansion demonstrates rapid evolution. Figure 11a shows the spectral shift to low frequencies ($f < 15$ kHz). The initial amplification at low frequencies followed by marked attenuation appears very similar to the 7-deg centered expansion (Fig. 5a). The streamwise coherence results just after the expansion display rapid development similar to the 7-deg centered expansion.

The similarity of the power spectra at $x/\delta_0 = 8.87$ (Fig. 11b) to that of the flat plate boundary layer is very misleading. Looking at the last measurement station in Figs. 12a and 12b, a substantial increase in the streamwise coherence across the entire frequency range is seen, whereas for the spanwise coherence an increase is observed at low frequencies. This indicates strong differences from the flat plate boundary layer are present, but there is no clear emergence of a band of new "structures" as for the 7-deg centered expansion. The streamwise and spanwise correlations, however,

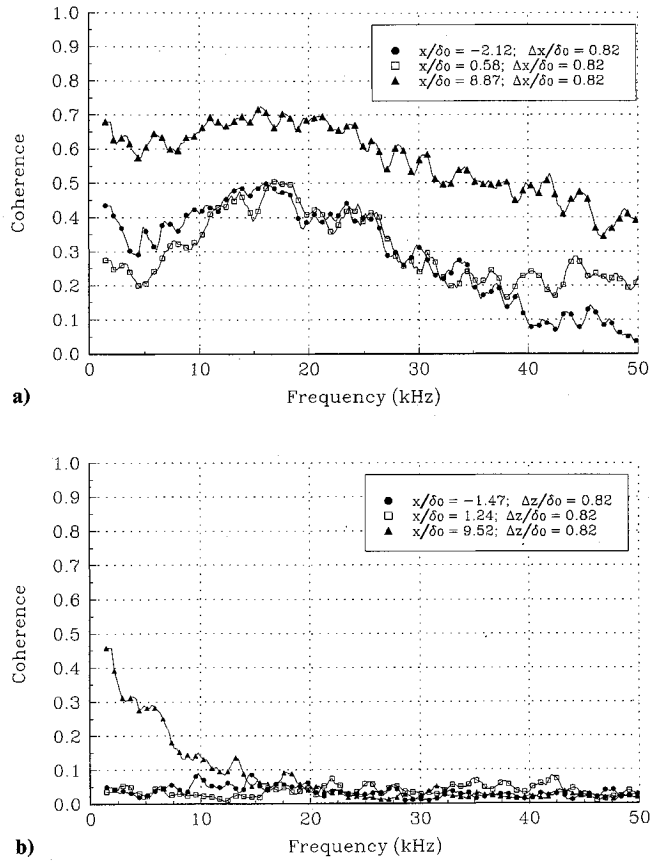

Fig. 12 Coherence downstream of the 14-deg centered expansion: a) streamwise and b) spanwise.

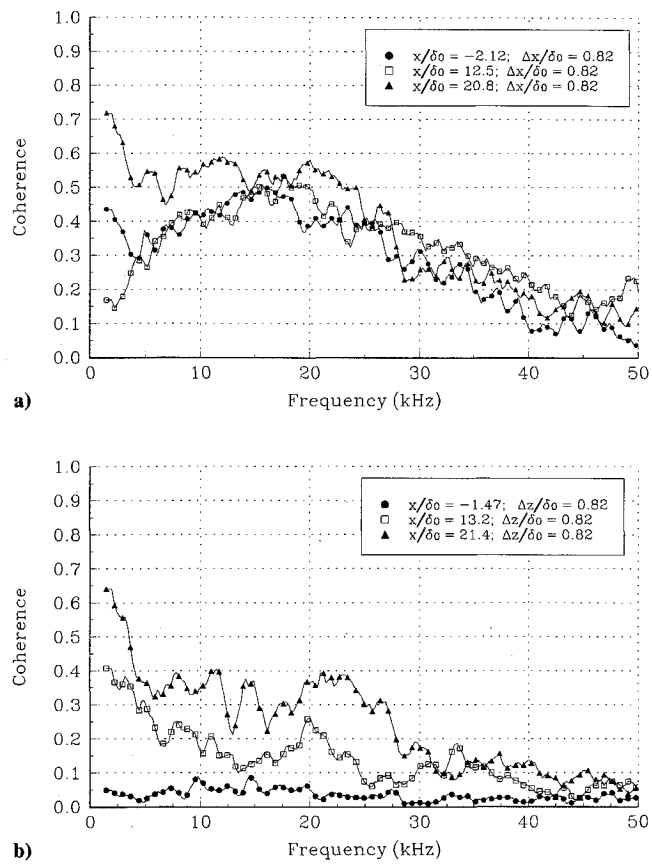

Fig. 13 Coherence downstream of the 14-deg gradual expansion: a) streamwise and b) spanwise.

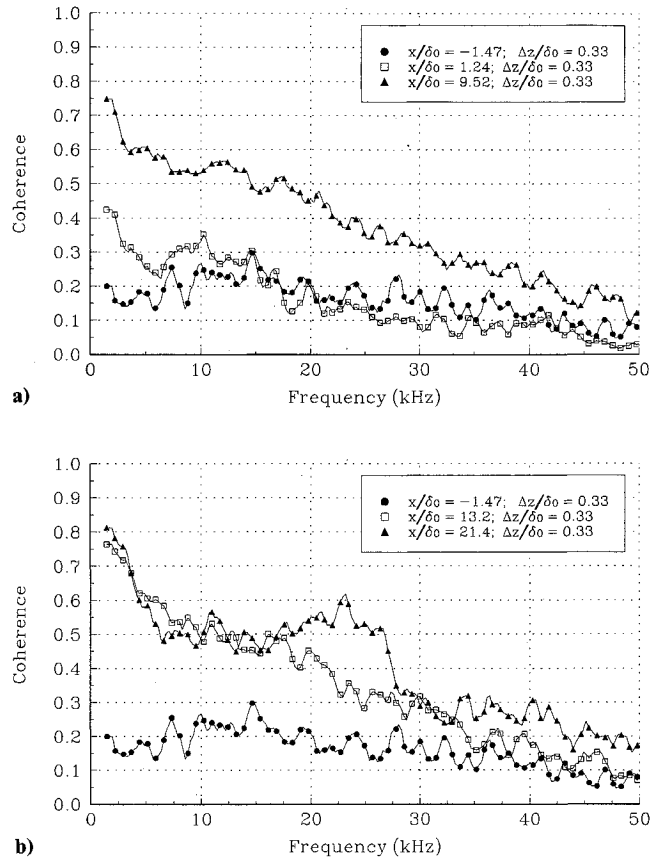

Fig. 14 Spanwise coherence downstream of 14-deg expansions: a) centered and b) gradual.

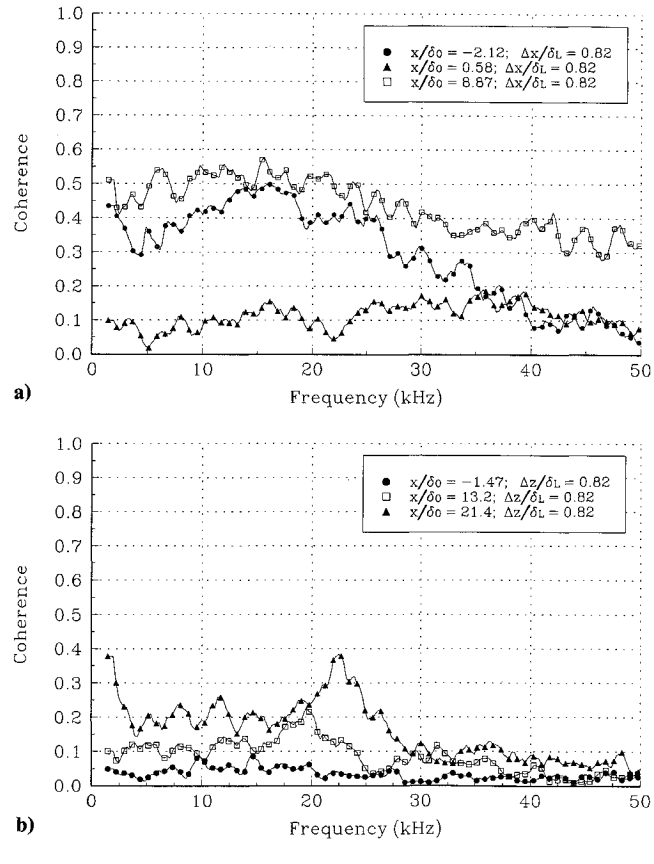

Fig. 15 Coherence downstream of 14-deg expansions with a transducer spacing of Δx(or z)/δ_L = 0.82 (normalized by local boundary-layer thickness): a) streamwise coherence, 14-deg centered expansion and b) spanwise coherence, 14-deg gradual expansion.

display a deviation from the flat plate correlations similar to the other expansions. The peak time delays in the space-time correlations again approach those of the incoming boundary layer with increasing downstream distance but remain far from the flat plate values at the last measurement location ($x/\delta_0 \simeq 9$). This again emphasizes that the boundary layer is quite different from the incoming boundary layer.

The emergence of the new features downstream of the 7-deg centered expansion is first apparent at $x/\delta_0 \simeq 10$ and is very noticeable at $x/\delta_0 \simeq 30$. The results indicate that the larger perturbation causes a more significant redistribution of the pressure fluctuations. As one would expect a longer period of adjustment for stronger perturbations, it may be expected that the emergence of any new structures would take longer for the 14-deg centered expansion. Since the last measurement station is at $x/\delta_0 \simeq 9$, it may be that the 14-deg centered expansion model is too short for the new structures to emerge. Merit for this idea is presented later.

D. 14-Deg Gradual Expansion

Similar to the 7-deg gradual expansion, the results for the 14-deg gradual expansion demonstrate that development just after the end of the expansion is not very rapid. However, the shift to low frequencies is much more noticeable than for the 7-deg gradual expansion as expected. Coherence results also display relatively slow development after the expansion.

As in both 7-deg expansions, the emergence of new structures is evident for the 14-deg gradual model. The downstream locations of Figs. 13a and 13b display a band of elevated coherence relative to the flat plate boundary layer. Again, the band is centered nominally at 20 kHz, suggesting that features similar to those of the 7-deg expansions have emerged.

Similar to the other expansions, coherence and space-time correlation levels at the last measurement location ($x/\delta_0 = 20.8$) are significantly larger than those of the incoming boundary layer. The peak time delays again evolve towards those of the flat plate boundary layer with increasing downstream distance, but very substantial differences are still present at $x/\delta_0 = 20.8$.

The coherence results for the 14-deg expansion models indicate the length of the 14-deg centered expansion model is too short for the development of the new structures. Comparing the farthest downstream measurement locations for these two models (Figs. 14a and 14b), it is obvious that the trends are the same, except that a peak around 15–30 kHz is superimposed on the spanwise coherence for the gradual case. Similar comparisons exist for the streamwise coherence at these locations. This shows that the development of the spanwise coherence is consistent for both 14-deg perturbations, but the extra length of the gradual expansion model allows the new features to emerge, whereas the centered model is too short.

Since the boundary-layer thickness increases across the expansion, using the pre-expansion value δ_0 as a global scale to normalize the transducer spacings might be questioned. Given the fixed transducer separations, one might wonder if the substantial increases in coherence and correlation levels sustained downstream of the expansions is not due mainly to the increase in boundary layer thickness. Figure 15 shows coherence results for $\Delta(x \text{ or } z)/\delta_L = 0.82$ where δ_L is the local boundary-layer thickness. Substantial increases in coherence with increasing downstream distance are still present, showing the increases in coherence and correlation levels are not simply a result of the δ_0 normalization. Similar trends are present for the correlation levels. Results are not given for the 7-deg cases because the fixed transducer separations did not afford similar δ_L-normalized separations at different locations.

IV. Conclusions

The results of this work indicate that the passing of a high-Reynolds-number Mach 3 turbulent boundary layer through centered or gradual ($R/\delta_0 \simeq 50$) expansions of 7 and 14 deg causes marked, long-lasting changes in the boundary-layer structure. The rms pressure fluctuations normalized by the local mean wall pressure remain nearly constant across all of the expansion regions. Normalized pressure spectra exhibit a shift to lower frequencies across the expansion, which is thought to reflect the quenching of small-scale, high-frequency motions by the dilatation associated with the expansion regions. This distortion of the spectra across the expansions is more significant for the 7-deg centered expansion than for the 14-deg gradual expansion but increases with total deflection for constant radius of surface curvature. The power spectra and spanwise coherence exhibit extremely fast development immediately after the centered expansions and relatively slow development immediately after the gradual expansions. For both the 7- and 14-deg cases, respectively, the structure of the boundary layer immediately after the gradual expansion region compares well with the structure of the boundary layer several boundary-layer thicknesses downstream of the centered expansion case, suggesting that the shorter "time of flight" through the centered expansions allows less boundary-layer adjustment. Streamwise space-time correlations in the perturbed boundary layers do not lend themselves to the derivation of convection velocities (although reasonable values are obtained in the flat plate boundary layer). New features appear at 15–30 kHz downstream of the expansions that are characterized by high levels of spanwise coherence and appear to give rise to spanwise correlation levels much higher than those of the flat plate boundary layer. Associated increases in streamwise coherence and correlation are not as pronounced. No strong evidence of a specific structural feature has been linked to these observations. The boundary-layer structure remained vastly different from that of the flat plate boundary layer at the last measurement locations, $x/\delta_0 \simeq 34$ (28) for the 7-deg gradual (centered) expansion and $x/\delta_0 \simeq 20$ (10) for the 14-deg gradual (centered) expansion.

Acknowledgments

The work was supported by the Air Force Office of Scientific Research (AFOSR-91-0412, monitored by L. Sakell). The helpful suggestions of a referee are greatly appreciated.

References

[1]Bradshaw, P., "The Effect of Mean Compression or Dilatation on the Turbulence Structure of Supersonic Boundary Layers," *Journal of Fluid Mechanics*, Vol. 63, Pt. 3, 1974, pp. 449–464.

[2]Spina, E. F., Smits, A. J., and Robinson, S. K., "The Physics of Supersonic Turbulent Boundary Layers," *Annual Review of Fluid Mechanics*, Vol. 26, 1994, pp. 287–319.

[3]Morkovin, M. V., "Effects of High Acceleration on a Turbulent Supersonic Shear Layer," Heat Transfer and Fluid Mechanics Inst., Stanford Univ., Stanford, CA, 1955.

[4]Lewis, J. E., Gran, R. L., and Kubota, T., "An Experiment on the Adiabatic Compressible Turbulent Boundary Layer in Adverse and Favorable Pressure Gradients," *Journal of Fluid Mechanics*, Vol. 51, Pt. 4, 1972, pp. 657–672.

[5]Thomann, H., "Effects of Streamwise Wall Curvature on Heat Transfer in a Turbulent Boundary Layer," *Journal of Fluid Mechanics*, Vol. 33, Pt. 2, 1968, pp. 283–292.

[6]Dussauge, J. P., and Gaviglio, J., "The Rapid Expansion of a Supersonic Turbulent Flow: Role of Bulk Dilatation," *Journal of Fluid Mechanics*, Vol. 174, 1987, pp. 81–112.

[7]Dussauge, J. P., "The Relaxation of a 'Relaminarized' Turbulent Boundary-Layer, in Supersonic– Flow," *Proceedings of the Fifth Symposium on Turbulent Shear Flows*, Cornell Univ., Ithaca, NY, 1985, pp. 2.27–2.31.

[8]Narasimha, R., and Sreenivasan, K. R., "Relaminarization in Highly Accelerated Turbulent Boundary Layers," *Journal of Fluid Mechanics*, Vol. 61, Pt. 3, 1973, pp. 417–447.

[9]Narasimha, R., and Viswanath, P. R., "Reverse Transition at an Expansion Corner in Supersonic Flow," *AIAA Journal*, Vol. 13, No. 5, 1975, pp. 693–695.

[10]Smith, D. R., and Smits, A. J., "The Rapid Expansion of a Turbulent Boundary Layer in a Supersonic Flow," *Theoretical and Computational Fluid Dynamics*, Vol. 2, 1991, pp. 319–328.

[11]Arnette, S. A., Samimy, M., and Elliott, G. S., "The Effect of Expansion on the Large Scale Structure of a Compressible Turbulent Boundary Layer," AIAA Paper 93-2991, July 1993.

[12]Samimy, M., Arnette, S. A., and Elliott, G. S., "Streamwise Structures in a Turbulent Supersonic Boundary Layer," *Physics of Fluids*, Vol. 6, No. 3, 1994, pp. 1081–1083.

[13]Samimy, M., Elliott, G. S., Glawe, D. D., Reeder, M. F., and Arnette, S. A., "Compressible Mixing Layers with and without Particles," Ohio

State Univ. TR MEMS-92-101, Columbus, OH, Aug. 1992.

[14]Jayaram, M., Taylor, M. W., and Smits, A.J., "The Response of a Compressible Turbulent Boundary Layer to Short Regions of Concave Surface Curvature," *Journal of Fluid Mechanics*, Vol. 175, 1985, pp. 343–362.

[15]Degani, D., and Smits, A. J., "Response of a Compressible, Turbulent Boundary Layer to a Short Region of Surface Curvature," *AIAA Journal*, Vol. 27, No. 1, 1989, pp. 23–28.

[16]Tan, D. K. M., Tran, T. T., and Bogdonoff, S. M., "Surface Pressure Fluctuations in a Three-Dimensional Shock Wave/Boundary Layer Interaction," AIAA Paper 85-0125, Jan. 1985.

[17]Fernholz, H. H., Finley, P. J., Dussauge, J. P., and Smits, A. J., "A Survey of Measurements and Measuring Techniques in Rapidly Distorted Compressible Turbulent Boundary Layers," AGARDograph No. 315, 1989.

[18]Corcos, G. M., "Resolution of Pressure in Turbulence," *Journal of the Acoustical Society of America*, Vol. 35, No. 2, 1963, pp. 192–199.

[19]Spina, E. F., Donovan, J. F., and Smits, A. J., "On the Structure of High-Reynolds-Number Supersonic Turbulent Boundary Layers," *Journal of Fluid Mechanics*, Vol. 222, 1991, pp. 293–327.

[20]Dawson, J. A., "An Experimental Investigation of Supersonic Turbulent Boundary Layers After an Expansion via Wall Pressure Measurements," M.S. Thesis, Dept. of Mechanical Engineering, Ohio State Univ., Columbus, OH, 1993.

[21]Muck, K. C., Dussauge, J., and Bogdonoff, S. M., "Structure of the Wall Pressure Fluctuations in a Shock-Induced Separated Turbulent Flow," AIAA Paper 85-0179, Jan. 1985.

[22]Lu, F. K., and Chung K., "Downstream Influence Scaling of Turbulent Flow Past Expansion Corners," *AIAA Journal*, Vol. 30, No. 12, 1992, pp. 2976, 2977.

[23]Lee, S., Lele, S. K., and Moin, P., "Simulation of Spatially Evolving Turbulence and the Applicability of Taylor's Hypothesis in Compressible Flow," *Physics of Fluids A*, Vol. 4, No. 7, 1992, pp. 1521–1530.

[24]Arnette, S. A., Samimy, M., and Elliott, G. S., "The Effect of Expansion on Large Scale Structure Evolution in a Compressible Turbulent Boundary Layer," AIAA Paper 94-2228, June 1994.